Published in Journal of Modern Optics 43, issue 7, 1473-1484, 1996
which should be used for any reference to this work

Diffractive optics for compact space communication terminals

P. BLATTNER, H. P. HERZIG, K. J. WEIBLE, J. M. TEIJIDO
Institute of Microtechnology, University of Neuchâtel,
rue A.-L. Breguet 2, 2000 Neuchâtel, Switzerland

H. J. HEIMBECK, E. LANGENBACH
Fisba Optik AG, Rohrschacherstrasse 268, 9016 St Gallen, Switzerland

and J. ROGERS
Leica Heerbrugg, 9435 Heerbrugg, Switzerland

Abstract. Free-space laser communication links with data rates between 10 and 500 Mbits s^{-1} are required to cover the large amount of communication needs between low-orbit satellites, geostationary satellites and ground stations. The objective of this paper is to demonstrate the potential of diffractive optical elements for the design of optical and optoelectronic systems for advanced laser communication terminals. Three different examples have been realized: a ring pattern generator, an athermalized and achromatic hybrid collimator system, and a hybrid beacon system.

1. Introduction

The design of first-generation free-space laser communication systems is based on laser diodes with output powers of the order of 100 mW [1]. The data rate transmission is of the order of 100 Mbits s^{-1}. This leads to terminals with large transmitter and receiver telescope diameters and, consequently, to high terminal mass and dimensions. The optical systems are usually designed with refractive lenses and reflective mirrors. Alternatives are planar diffractive optical elements (DOEs). By relying on diffraction and interference rather than on reflection and refraction, unique and novel properties can be realized. Almost any structure shape, including non-rotationally symmetric aspherics, can be manufactured, which provides all degrees of freedom for the design. Other interesting aspects of DOEs are their low weight, their strong dispersion, and the possibility of making segmented elements, large arrays of elements, beam splitters and polarizers. These properties are useful for many applications of DOEs in space, including filters for image data processing [2], beam shaping [3, 4] and antireflection structures [5, 6]. Furthermore, the combination of refractive and diffractive surfaces (hybrid elements) offers new possibilities for optical design. The negative dispersion of DOEs can be used to compensate the chromatic aberrations of refractive lenses [7, 8]. Hybrid elements can also be used to compensate the

temperature-induced variations in their mounting system. Some examples of athermalized hybrid lenses have been discussed in the literature [9, 10]. DOEs for space applications must comply with a number of requirements, including mechanical, thermal and optical stability [8]. Suitable techniques for realizing the microstructures in space-qualified materials are based on a variety of high-resolution lithographic and optical processes [11].

In this paper, we discuss possible applications for DOEs in compact optical communication terminals. The design and experimental realization of three different elements are presented. These elements include a ring pattern generator allowing tracking and data transmission within one optical element, an athermalized hybrid achromat and a hybrid lens system.

2. Free-space laser communication terminals

Figure 1 shows as an example the design of the optical head of the very small optical user terminal (VSOUT) discussed in [1]. The head consists of two units: an optical block and a mirror pointing assembly attached to the optics block. The optics block is made up of the laser transmitter assembly, the acquisition sensor, the tracking–receiver combination, the telescope and the associated beam-forming optics. A beacon system (generating a large divergent beam) is mounted at the outer coarse pointing mirror housing and is connected to a high-power laser package with a fibre. Many potential applications for DOEs exist in such a system, as follows.

(1) *Laser diode transmitters.* High-power light sources allow long communication distance; a beam-shaping DOE could be used to collimate the output beams of a high-power laser diode array.

(2) *Telescope system.* Complex telescope systems may be simplified using DOEs; the DOEs allow one to reduce the number of elements; furthermore, all lenses could be fabricated with the same material.

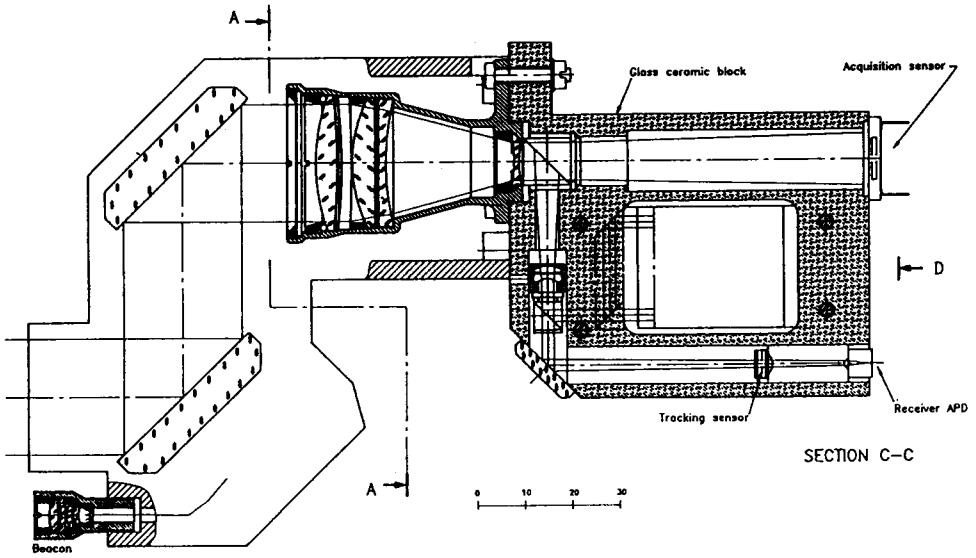

Figure 1. Very small optical user terminal (VSOUT): optical head design.

(3) *Tracking–receiver system.* DOEs allow multitasking with a single element; the tracking and receiving function could be realized by a segmented element.
(4) *Collimator of the beacon head.* The system can be simplified by hybrid (refractive–diffractive) elements.
(5) *Beam splitter.* Multiple beam splitting can be done with one DOE; the number of beam-splitting elements and their weight could be reduced.

In the following, a detailed description of the design of the DOEs used in the tracking–receiver system, an athermalized hybrid collimator, as well as the hybrid beacon system is given. All three elements have been realized by lithography and subsequent etching. The procedure is to generate a mask by electron beam or laser beam lithography. Then, the mask is transferred into an eight-level surface-relief structure by dry etching in fused silica or optical glass.

2.1. *Tracking–receiver system*

A schematic diagram of the tracking–receiver system [12] of the VSOUT optical head is shown in figure 2. The tracking sensor consists of a four-quadrant detector with a central hole which acts as a field stop for the subsequent receiver optics. The specific task of the diffractive optical element, situated at the entrance of the tracking–receiver system, consists of focusing the incoming beam into the central hole (receiver signal) while generating a ring intensity pattern in the tracking detector plane (tracking signal). Changes in the relative positions of the sending and receiving communication terminals are directly translated into a shift of the ring intensity pattern on the tracking sensor, which can be measured by means of the four-quadrant detector.

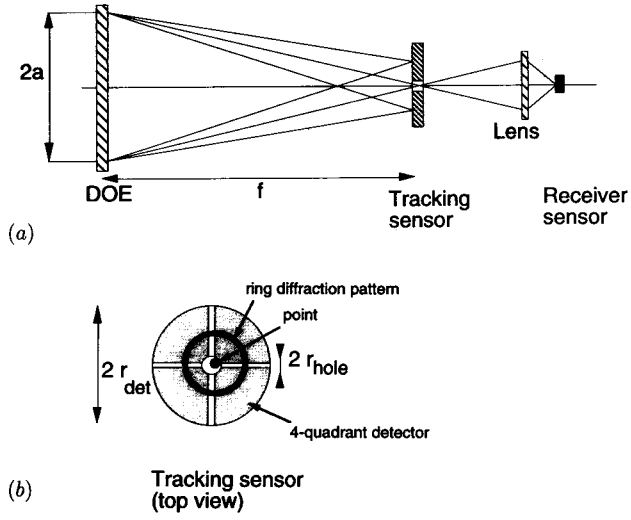

Figure 2. Principles of the tracking–receiving system: (*a*) side view; (*b*) top view. Changes in the relative positions of the sending and receiving communication terminals are directly translated into a shift of the ring intensity pattern on the tracking sensor, which can be measured by means of the four-quadrant detector.

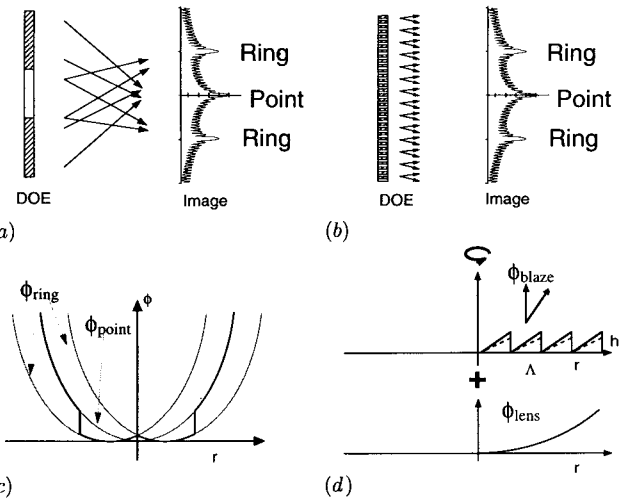

Figure 3. Two different design approaches for the tracking–receiver element: (*a*) segmented aperture design; (*b*) common aperture design; (*c*) the phase function of the segmented element; (*d*) the phase function of the common aperture element.

Different design methods exist for the tracking–receiver DOE. The two specific tasks may be made by a segmented element, which means that the surface of the DOE is divided into two parts: a simple lens function in one part for the focusing point, and a radially shifted lens function in the other part for generation of the ring pattern (segmented aperture design). An alternative technique is to generate the ring pattern by the first diffraction order of a rotational blazed grating structure combined with a focusing function. The focal point in the centre is then realized by the zero order of the grating structure. In this case, both functions are generated by the whole element and thus have the same aperture (common aperture design). The two design strategies are shown in figures 3 (*a*) and (*b*).

DOEs are mainly described by their phase function. For the segmented elements, each segment has its own phase function. In the case of the tracking–receiver DOE the phase function ϕ is then given by

$$\phi(r) = \begin{cases} -\dfrac{k}{2f} r^2, & \text{for } r_{seg} < r < a, \\ -\dfrac{k}{2f}(r - r_{ring})^2, & \text{for } 0 < r < r_{seg}, \end{cases} \tag{1}$$

where k is the wave-vector, f the focal length of the tracking system, r_{ring} the radius of the ring intensity pattern on the four-quadrant detector, $2a$ the diameter of the DOE, and r_{seg} the radius of separation of the two different segments. The function $\phi(r)$ is shown in figure 3 (*c*). The advantage of this concept is that the ratio of the energy used for tracking (ring) to the energy used for the receiver (focal point) is directly given by the ratio of the surfaces of the two segments (i.e. $(r_{seg}/a)^2$). Furthermore, the two optical functions can be tested and characterized independently by covering one of the segments. However, a drawback of this concept might be that the system is not shift invariant, that is a change in the input

intensity distribution directly affects the output functions. Also, the radius of the diffraction spot of the focus and the width of the ring are given by the aperture of the corresponding segments. This can lead to design problems. In particular, if much more energy has to be in the central point than in the ring, the surface of the segment used to generate the ring becomes small; thus the width of the ring becomes very large owing to diffraction. On the other hand, if much more energy has to be in the ring than in the point, the point becomes very large. Depending on the design specifications the segmented approach may not be satisfying. The above-mentioned problem can be avoided by the common aperture design.

The phase function of the common aperture design is composed of a lens function and a blazed grating structure defined over the entire aperture:

$$\phi(r) = -\frac{k}{2f}r^2 + h \bmod \left(\frac{r}{\Lambda}, 1\right), \tag{2}$$

where Λ is the period of the grating structure, h is the phase depth of the grating structure and mod (a, b) is the modulo function (also referred to the fractional part of the division a/b). The phase function $\phi(r)$ is shown in figure 3 (d). The grating period Λ determines the beam deflection of the first diffraction order and thus the radius of the ring, while the phase depth h of the grating structure determines the energy distribution in the different diffraction orders. The diffraction efficiency of the first order of a blazed phase grating is given by

$$\eta_1 = \sin^2\left(\frac{h}{4}\right). \tag{3}$$

For a 2π-deep blaze structure, only the first diffraction order has energy; only a ring structure without a central peak is generated. If the phase depth differs from 2π, then the zero order will also gain some energy, but also higher orders appear, that is rings of radius $2r_{\text{ring}}$, $3r_{\text{ring}}$, etc., are created. However, these higher-order rings do not affect the functionality of the tracking system. In this approach the diameter of the diffraction spot is given by the aperture of the whole DOE and is therefore smaller than in the first approach.

Based on the design of the VSOUT a ring generator has been fabricated. The specifications of the element are as follows: the design wavelength is 818 nm, the focal length of the element is 20 mm, the diameter of the DOE is 2 mm, and the diameter of the central hole in the tracking detector is 0·1 mm. Furthermore, 75% of the energy has to be inside the central hole of the tracking detector used for the receiver. The resulting eight-phase level element has smallest features of the order of 2 μm. The DOE was realized in fused silica. In addition, a set of visible light demonstrators (633 nm) for the ring–point generation has been made, with a focal length of 400 mm and a diameter of the generated ring of 15 mm. For these demonstrators, both design approaches have been tested. Figure 4 (a) shows the diffraction pattern of the common aperture design. Scans through the focus in the image plan, together with the calculated function are presented in figures 4 (b) and (c) for the segment aperture and the common aperture design respectively. The measured intensity distribution shows excellent agreement with the expected theoretical data. The difference between theory and measurements can be explained by etch depth errors in the fabrication.

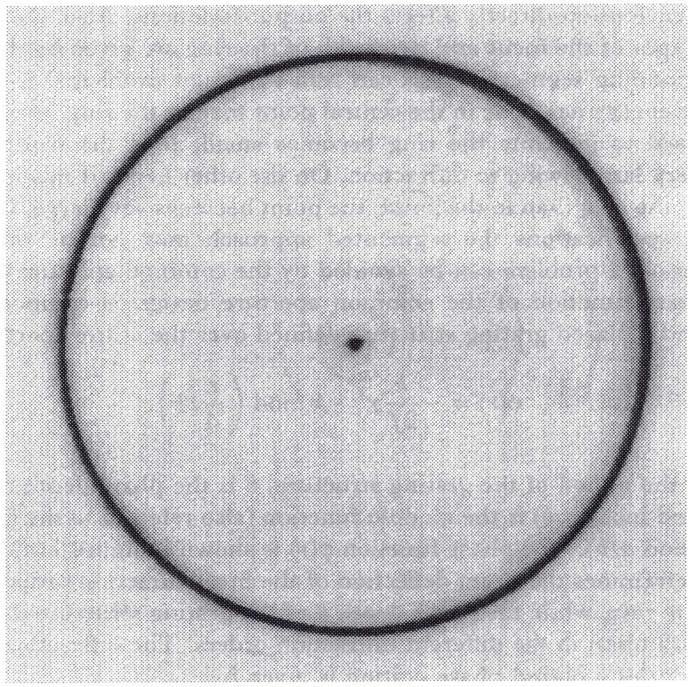

(*a*)

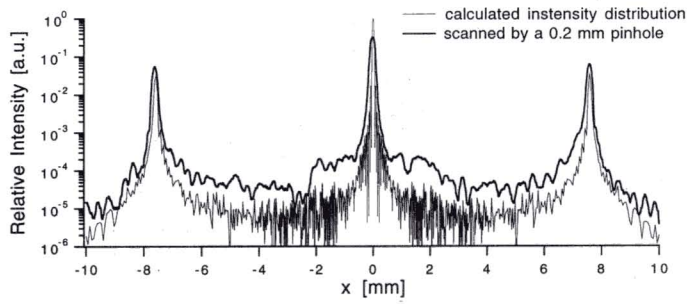

(*b*)

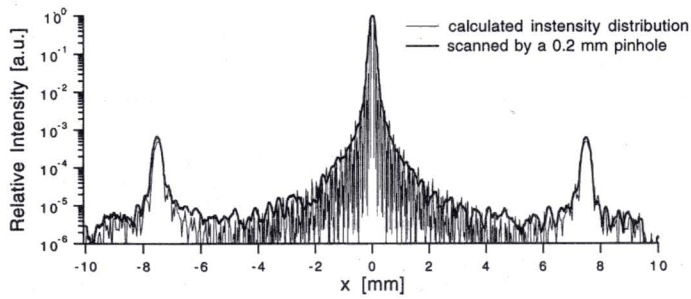

(*c*)

Figure 4. (*a*) The diffraction pattern of the common aperture design. (*b*), (*c*) Scans through the focus in the image plan, together with the calculated curves (*b*) for the segment aperture and (*c*) for the common aperture design (a.u., arbitrary units).

2.2. *Athermalized and achromatic hybrid collimator system*

Space environment introduces severe conditions for the thermal behaviour on the used elements. For this purpose an athermalized achromatic system has been designed, which keeps the position of the focal point within a small region when operating temperature and illumination wavelength is changing. The negative dispersion associated with the DOE is used to compensate the chromatic aberrations of the refractive lens, while the thermal properties of the optical material are exploited to compensate the thermally induced expansion of the supporting mount.

In particular, the dispersion of the DOE is negative, stronger and material independent compared with the refractive element. An achromat can therefore be designed with two focusing elements, contrary to a traditional achromatic doublet, where one of the two refractive elements needs negative power for the chromatic compensation. Consequently, the focusing power of the other refractive element has to be higher; thus the magnitude of the higher-order aberrations are larger in the classical design. Furthermore, the hybrid achromat can be designed with the same material which simplifies also the design of a thermally compensated system.

For such an athermalized system the variation of the mounting has to be compensated by the focal length variation of the optical system (figure 5). The focal length variations are described by an optothermal expansion coefficient, the mechanical variations in the mounting material by a thermal expansion coefficient. The general approach for the design of an athermalized system is to choose correctly the glasses and the mounting materials so that these expansion coefficients are equal [13]. Once the appropriate glass and mounting material has been determined, the optical design is made. In this design the DOE element is consdered as an ultra-thin lens with a very high refractive index, referred to as the high-refractive-index (HRI) model [8, 13]. The attractive feature of this model

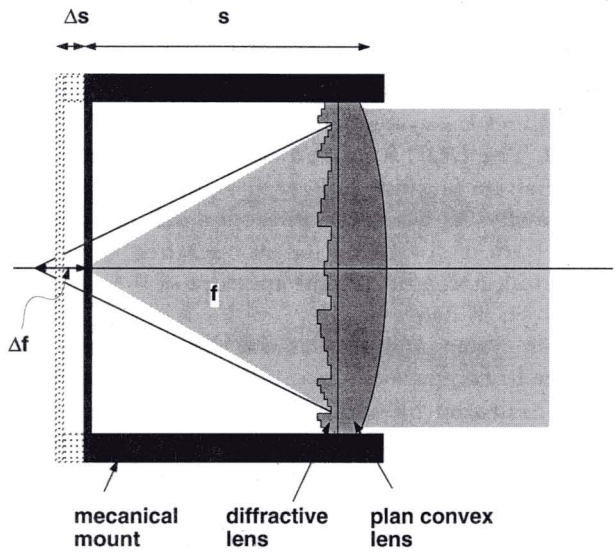

Figure 5. Athermalized achromat, together with its mounting mechanics. For an athermalized element the displacement Δs introduced by the supporting mount has to be compensated by the thermal variation Δf in the focal length.

is that DOEs can be represented in any lens design software as arbitrary aspherics, which in turn are realized directly by standard DOE manufacturing processes.

A hybrid collimator of 5·2 mm diameter and 8 mm focal length has been designed and fabricated. The system is thermally compensated for a range from −20 to 40°C and has a working wavelength range 630–670 nm. The mount material is a combination of aluminium and steel which has a thermal expansion coefficient of $26{\cdot}4 \times 10^{-6}°C^{-1}$. It has been found that FK51, which has an optothermal expansion coefficient of $25 \times 10^{-6}°C^{-1}$, is an appropriate glass in order to satisfy the athermalization condition. The length variation of the mount is 11 μm over the whole temperature range; the calculated shift Δf of the focal length of the hybrid system is 12·6 μm. Hence, the absolute change in the focal point position is less than 2 μm. The designed DOE has been realized in FK51 by photolithography and ion beam milling. The resulting eight-phase level element has smallest features in the order of 3 μm. A good criterion to judge the performance of the collimator is to measure the wave-front aberrations of the system. Figure 6 (*a*) shows the expected optical path difference for the central design wavelength of 650 nm and the measurement wavelength of 633 nm and figure 6 (*b*) shows a double-pass interferogram of the hybrid collimator at 633 nm. The central fringe of the measured double-pass interferogram behaves exactly as the calculated values. The expected maximal optical path difference is of the order of $\lambda/4$ which corresponds nicely to the shift of $\lambda/2$ in the measured double-pass interferogram.

2.3. *Hybrid beacon system*

The third selected application for DOEs is the collimator for the beacon system. The task of the beacon system is to generate a large divergent beam, which is used in a pre-operational phase of the communication link in order to locate the opposite communication terminal. In the classical VSOUT design the beacon system consists of four refractive lenses (figure 7 (*a*)) of different glass types. The benefit of a hybrid design is the reduction in the number of elements, namely from four elements of different materials to three elements of the same material, which simplifies the system and lowers its weight. The hybrid system is shown in figure 7 (*b*). The DOE is located at surface 3. Note that the planar back side of the DOE substrate (surface 2) is used as protection of the optical system and can be cleaned easily. As described in section 2.2, the design is based on the HRI model. The system is optimized for an operating wavelength of 850 nm, a focal length of 6·25 mm, and a numerical aperture of 0·4. The resulting aspheric phase function is shown in figure 8.

The hybrid beacon system and the classical beacon system have been designed and realized in order to compare the two different approaches. The DOEs were manufactured by a multistep lithographic process in fused silica for a working wavelength of 850 nm. The smallest structure for an eight-level element is in the order of 6 μm. Figure 9 shows the calculated wave-front aberrations for both systems. It can be seen that the hybrid design shows even less aberrations than the classical design. The wave front of the classical and the hybrid design were measured and compared at 633 nm. The expected peak-to-valley wave-front error at this wavelength turns out to be $0{\cdot}2\lambda$ for the classical and $1{\cdot}6\lambda$ for the hybrid system. The measured values are 0.32λ and $1{\cdot}29\lambda$. Thus the measurements are in

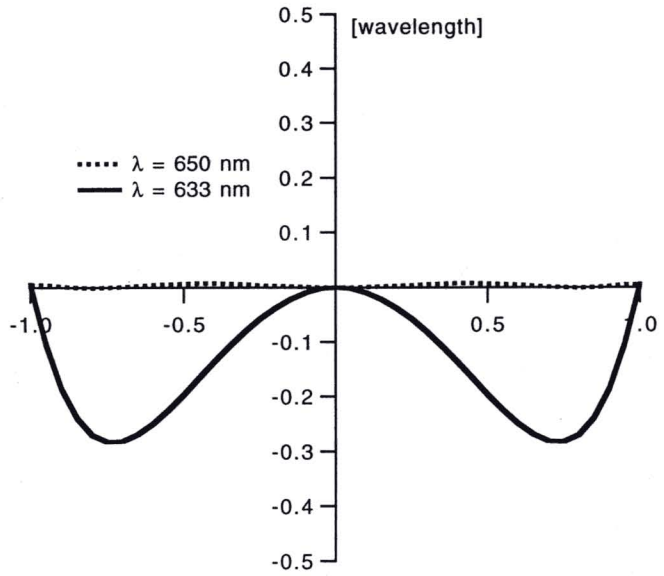

(*a*)

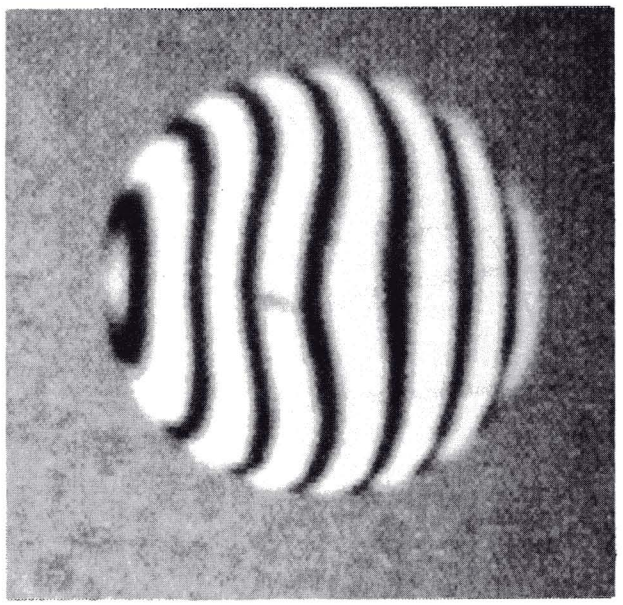

(*b*)

Figure 6. (*a*) Expected optical path difference of the achromatic system for $\lambda = 633$ nm. (*b*) Double-pass interferogram of the realized system at this wavelength. The measurement shows exactly the calculated behaviour.

agreement with the theoretical values, the differences are explained by misalignment errors.

3. Conclusions

It has been shown that there is a large potential for diffractive optical elements in optical space communication terminals. The system design with the help of

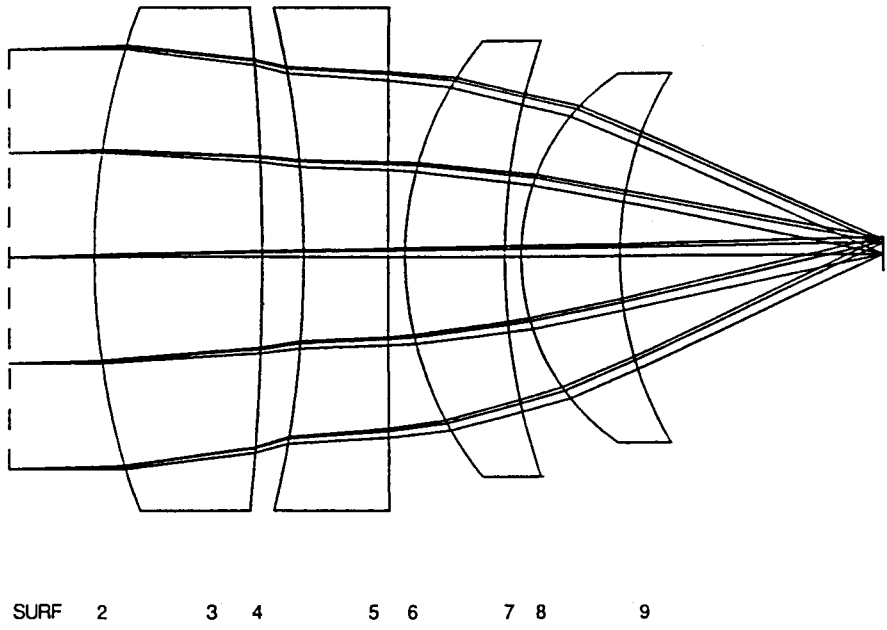

(*a*)

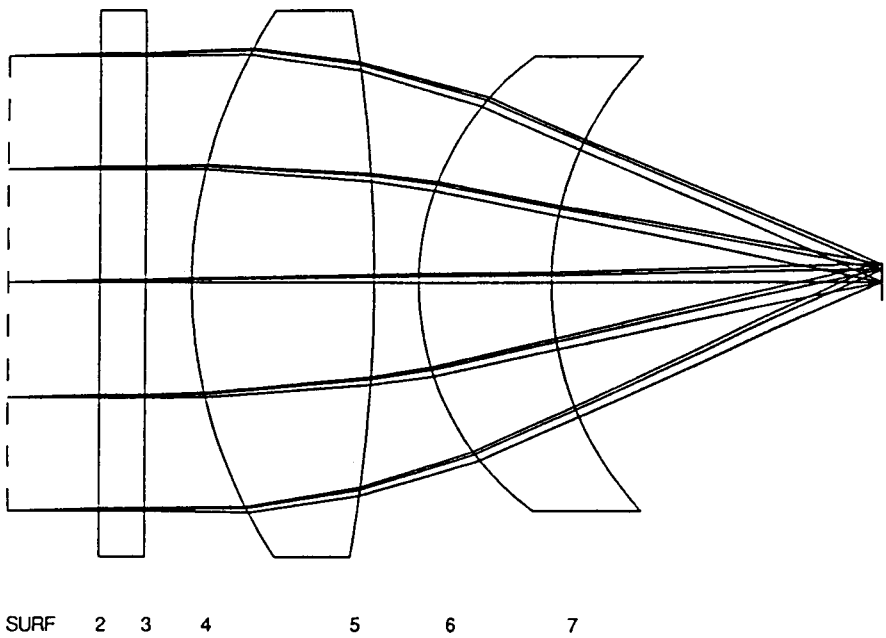

(*b*)

Figure 7. Beacon system: (*a*) classical design; (*b*) hybrid design.

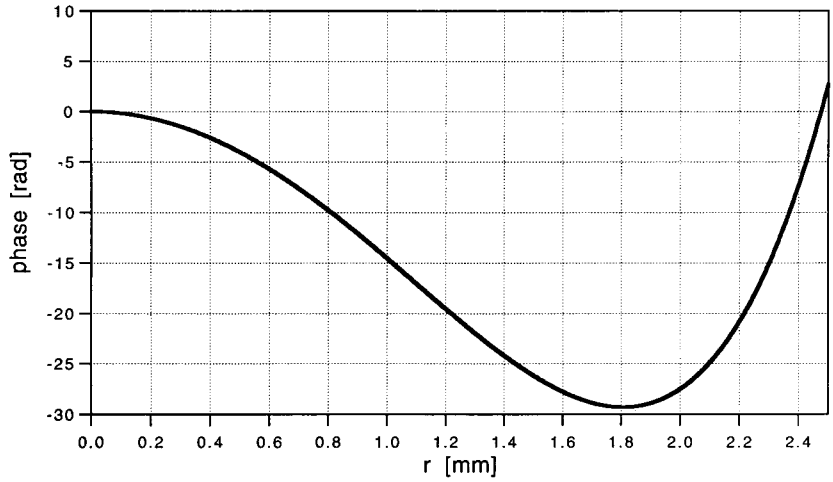

Figure 8. Phase function of the DOE for an optimized beacon collimator with a numerical aperture of 0·4 and a focal length of 6·25 mm.

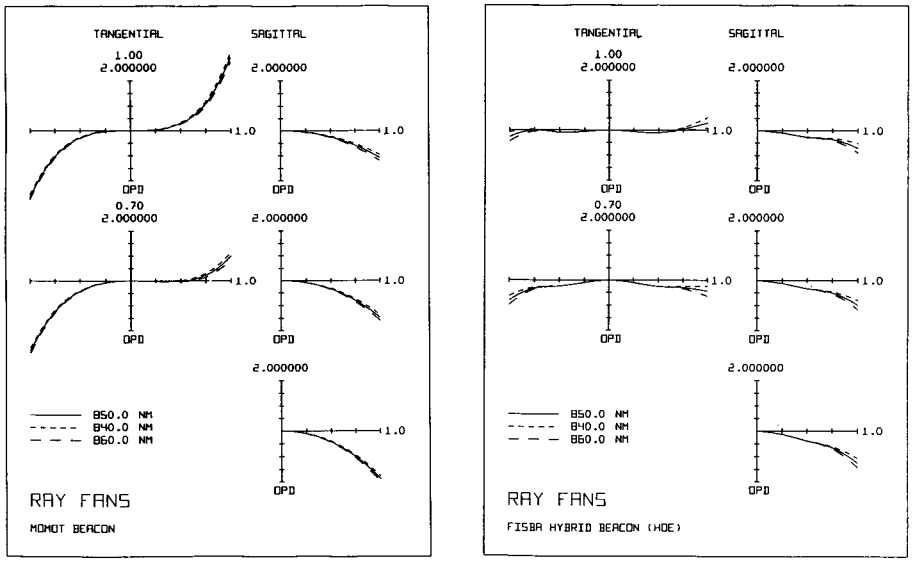

(*a*) (*b*)

Figure 9. Expected wave-front aberration of the beacon collimator for (*a*) a classical design and (*b*) a hybrid design.

DOEs benefits from all the main advantages of these elements in order to reduce complexity, weight and costs. Three different systems using diffractive optics have been selected at the example of the VSOUT. First, a tracking–receiver system has been discussed where both functionalities were performed by a single DOE. The task of this DOE is to generate a point–ring pattern. For this purpose, two different design strategies have been investigated. One is based on a segmented aperture, and the other on a common aperture approach. The realized elements showed good agreement with the theory for both types of design. However, it

turned out that the segmented aperture-based system may give some problems for specific point–ring energy ratios. Secondly, the design and realization of an athermalized and achromatic hybrid collimator system have been presented. The performance of this system is in excellent agreement with the expected theoretical values. Third, a hybrid beacon system has been presented consisting of one diffractive and two refractive elements. It has been shown that it is possible to reduce the complexity of a classical system by introducing DOEs while keeping the same optical performances. All elements have satisfied the given severe specifications for space applications, which encourages the use of DOEs in other systems in the near future.

Acknowledgments

Parts of this work have been done in the framework of the ESA project No. Col0566/93/NL/JV and of the Swiss priority program 'Optique'.

References

[1] Czichy, R. H., and Wittig, M., 1993, *Proceedings of the Conference on Holographic Systems, Components and Applications*, Neuchâtel, 1993, IEE Conference Publication No. 379 (London: Institution of Electrical Engineers), pp. 255–259.
[2] Wyrowski, F., 1991, *Appl. Optics*, **30,** 4650–4657.
[3] Eisenmann, M. T., Tai, A. M., and Cederquist, J. N., 1989, *Appl. Optics*, **28,** 2641–2650.
[4] Ehbets, P., Herzig, H. P., Dändliker, R., Regnault, P., and Kjelberg, I., 1993, *J. mod. Optics*, **40,** 637–645
[5] Ono, Y., Kimura, Y., Ohta, Y., and Nishida, N., 1987, *Appl. Optics*, **26,** 1142–1146.
[6] Raguin, D., and Morris, G. M., 1993, *Appl. Optics*, **32,** 2582–2598.
[7] Stones, T., and George, N., 1988, *Appl. Optics*, **27,** 2960–2971.
[8] Czichy, R. H., 1993, *Hybrid Optics for Space Applications*, ESA Scientific/Technical Monographs No. SP-1158 (Noordwijk: ESA Publications Division).
[9] Behrmann, G. P., and Bowen, J. P., 1993, *Appl. Optics*, **32,** 2483–2489.
[10] Londoño, C., Plummer, W. T., and Clark, P. P., 1993, *Appl. Optics*, **32,** 2295–2302.
[11] Herzig, H. P., Gale, M. T., Lehmann, H. W., and Morf. R., 1993, *Perspectives for Parallel Interconnects*, edited by Ph. Lalanne and P. Chavel (Berlin: Springer).
[12] Czichy, R. H., 1992, ESA/PAT/274.
[13] Jamieson, T. H., 1981, *Opt. Engng*, **20,** 156–160.
[14] Sweatt, W. C., 1979, *J. opt. Soc. Am.*, **69,** 486–487.